doi:10.1017/S143192761900237X
Microsc. Microanal. 25 (Suppl 2), 2019

Investigation of Microstructure and Dispersoids/Precipitates in Additively Manufactured Aluminum Alloys

L. Zhou[1*], H. Hyer[1], S. Park[1], Y. Sohn[1], KP. Rice[2], Y. Chen[2]

[1.] Advanced Materials Processing and Analysis Center, Department of Materials Science and Engineering, University of Central Florida, Orlando, FL, 32816, USA
[2.] CAMECA Instruments Inc., 5470 Nobel Dr, Madison, WI, 53711, USA
* Corresponding author: le.zhou@ucf.edu

Additive manufacturing (AM) of metallic alloys is becoming an increasingly important area of interest for academia and industry due to its method of fabricating components with highly complex or customized geometries. The complicated thermo-kinetic environment associated with AM is challenging for many traditional materials, particularly aluminum-based alloys. Currently, many Al alloys manufactured by AM are Al-Si alloys near the eutectic composition, while high strength 7xxx series alloys tends to exhibit excessive solidification cracking [1]. However, opportunities are emerging in the design of novel Al alloys that are suitable for AM and take advantage of the AM process.

Recent advancements in novel high-strength Al alloy design for AM involves the proper alloying of Sc or Zr [2]. It has been demonstrated that the new high strength AlZnMgScZr alloys exhibited outstanding tensile strength and elongation [2]. The alloying of Sc or Zr contributes to the grain refinement in the as-built alloy and precipitation hardening during the subsequent heat treatment. This work investigates the microstructure and dispersoids/precipitates in additively manufactured AlZnMgScZr alloys in detail through various characterization techniques.

The AlZnMgScZr alloys were manufactured by laser powder bed fusion (LPBF) using a SLM® 125HL (SLM Solutions, Germany). The powders were prepared using a gas atomization system (Dong Yang Induction Melting Furnace Co Ltd, Korea). The as-built and heat-treated samples were metallurgically prepared and characterized by optical microscope, scanning electron microscope (FE-SEM, Zeiss Ultra-55), electron backscatter diffraction (EBSD, EDAX Hikari camera, TEAM software), transmission electron microscope (TEM, FEI/Tecnai™ F30 300 kV) and atom probe tomography (APT), (EIKOS-X).

Fig.1(a) shows the EBSD inverse pole figure (IPF) map of the as-built AlZnMgScZr alloy. The as-built AlZnMgScZr alloy exhibits a fine bimodal grain morphology, with tiny equiaxed grains along the melt pool boundaries and small columnar grains within the melt pools. A representative high angle annular dark field (HAADF) micrograph from the equiaxed grain region is shown in Fig.1(b), where multiple dispersoids formed during solidification were observed both within the grains and along the grain boundaries. These dispersoids include MgZn, Al_3Sc and some Fe-rich intermetallics. Elemental distribution from APT analysis of a triple junction is shown in Fig. 1(c), which indicates that the grain boundary is slightly depleted in Zn and Mg with Sc-enriched dispersoids along the grain boundaries

Fig. 2 shows the precipitation analysis from TEM and APT for the heat-treated AlZnMgScZr alloy. The heat treatment is carried out following the conventional T6 heat treatment, which consists of a solution heat treatment at 480 °C for 1 hour and aging at 120 °C for 24 hours. Both precipitates of Al_3Sc and η'-$MgZn_2$ have been identified in the heat-treated alloys. The average diameter of the Al_3Sc and η'-$MgZn_2$ is 11.0 nm and 2.8 nm, respectively. The size and distribution of η'-$MgZn_2$ is ideal for obtaining maximum precipitation strengthening [3], however, the size of Al_3Sc is too coarse to obtain maximum precipitation strengthening [4]. This indicates that the optimal precipitation hardening cannot be obtained with the conventional T6 heat treatment for this alloy. Strategies for hardness optimization is needed and will be discussed.

References:

[1] JH Martin et al., Nature **549** (2017), p. 365.
[2] L Zhou et al., Scripta Materialia **158** (2019), pp. 24-28.
[3] M Nicolas, and D Alexis, Acta Materialia **51** (2003), pp. 6077-6094.
[4] DN Seidman, EA Marquis, and DC Dunand, Acta Materialia **50** (2002), pp. 4021-4035.

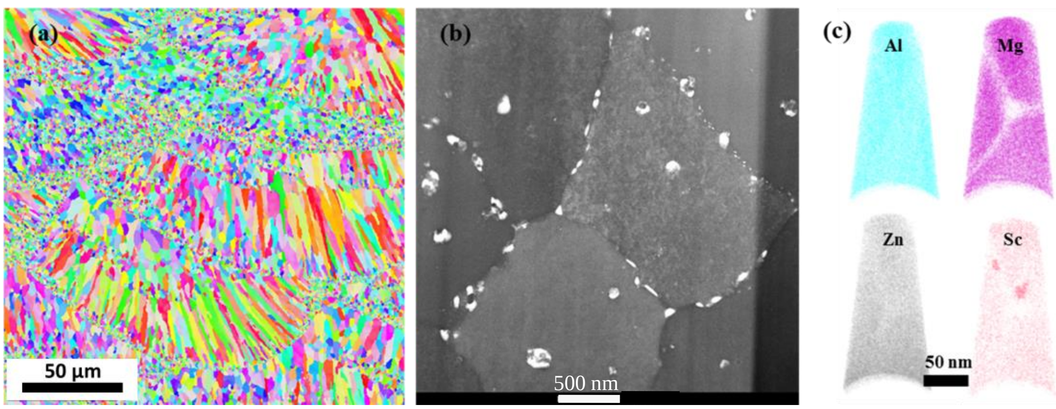

Fig. 1. (a) EBSD grain orientation mapping for laser powder bed fused AlZnMgScZr alloys. (b) HAADF micrograph of the equiaxed grain region along the melt pool boundary. (c) APT ion maps showing the elemental distribution of Al, Zn, Mg and Sc near a triple junction.

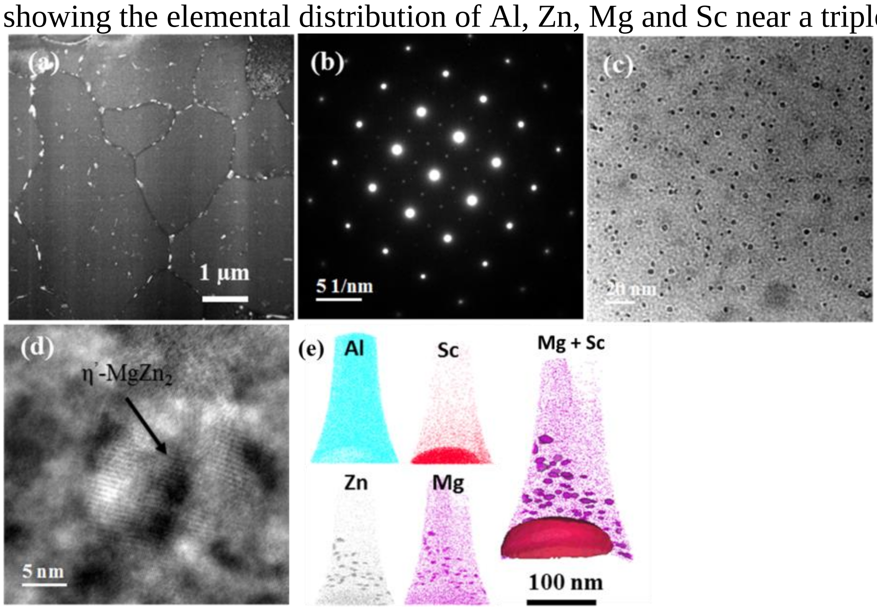

Fig. 2. (a) HAADF micrograph of the heat-treated AlZnMgScZr alloy. (b) Selected area diffraction pattern from [001] orientation of the matrix. (c)-(d) High resolution TEM micrographs showing the precipitates of η'-$MgZn_2$ and Al_3Sc. (e) APT ions maps of the elemental distribution in AlZnMgScZr.

https://doi.org/10.1017/S143192761900237X Published online by Cambridge University Press